Comparison of the global TRMM and WFD precipitation datasets in driving a large-scale hydrological model in southern Africa

Lu Li, Cosmo S. Ngongondo, Chong-Yu Xu and Lebing Gong

ABSTRACT

This paper provides a comparison of two widely used global precipitation datasets in southern Africa: Tropical Rainfall Measuring Mission (TRMM) and Water and Global Change (WATCH) Forcing Data (WFD). We also evaluate the performance of the water and snow balance modelling system (WASMOD-D) in a water balance simulation of 22 gauged basins over the southern Africa region. Water balance for southern Africa was simulated using the two global datasets as input with regionalized model parameter values. The results reveal that the special variation patterns of mean annual precipitation from TRMM and WFD datasets and temporal changing trend are similar in southern Africa. However, they are quite different in terms of probability distributions. Simulation of WASMOD-D based on two datasets in southern Africa results in model performances of above 0.5 for Nash–Sutcliffe (NS) values, below 10% for volume error (VE) values and a good reproduction of the observed flow duration curves for the majority of the basins. Finally, WFD data which have been bias corrected were observed to outperform TRMM data in southern Africa. The approaches and results described in this study contribute to the limited literature on regional hydrological modelling in the data-scarce region of southern Africa.

Key words | large-scale hydrological model, precipitation, southern Africa, TRMM, WATCH Forcing Data, water resources

Lu Li (corresponding author)
Cosmo S. Ngongondo
Chong-Yu Xu
Lebing Gong
Department of Geosciences,
University of Oslo,
PO Box 1047 Blindern,
N-0316 Oslo,
Norway
E-mail: *lu.li@geo.uio.no*

Cosmo S. Ngongondo
Department of Geography and Earth Sciences,
University of Malawi,
Chancellor College,
PO Box 280, Zomba,
Malawi

Chong-Yu Xu
Department of Earth Sciences,
Uppsala University,
Sweden

Lebing Gong
Department of Physical Geography and Quaternary Geology,
Bert Bolin Centre for Climate Research,
Stockholm University,
Stockholm,
Sweden

INTRODUCTION

In recent years, large-scale hydrological models have increasingly been used as a main assessment tool for global/regional water resources. Many large-scale hydrological models have been developed to estimate present and future water resources at large scales for the purposes of, for example, climate change impact (Arnell 1999, 2004; Vörösmarty *et al.* 2000; Nijssen *et al.* 2001; Lehner *et al.* 2006; Yang *et al.* 2012), water resources assessment (Doll *et al.* 2003), transboundary water management (Furlong 2006; Heyns *et al.* 2008; Arheimer *et al.* 2012) and virtue water trading (Islam *et al.* 2007). With technological advancements, high-resolution and high-quality global topographical and hydrographical data are currently available. Discharge data are still the base for global/regional water resources assessment today.

Large-scale hydrological modellers face many challenges in modelling. First, much of the Earth's land surface is covered with un-gauged basins. For some gauged basins, especially in developing regions such as Africa, the problem is the low data quality and availability (Jung *et al.* 2012). This results in large uncertainties and errors during calibration and simulation (Beven & Freer 2001; Refsgaard *et al.* 2007; Hughes 2011; Adeloye & Rustum 2012), i.e. determining unphysical parameter values in modelling, or using runoff-correction factors in order to reproduce the observed discharge (Fekete *et al.* 2002; Doll *et al.* 2003). Second, another problem is flow predictions in un-gauged basins using information from the gauged basins (Todini 2011). The lack of data for calibration and verification makes

doi: 10.2166/nh.2012.175

prediction in un-gauged basins very challenging, and this is considered as one of the major issues in hydrological sciences (Burn & Boorman 1993; Sivapalan *et al.* 2003).

For the first problem, if observation periods of the input and output data do not overlap, traditional model calibration criteria such as the Nash–Sutcliffe coefficient (NS) and determination coefficient (R^2), which rely on the comparison of simulated and observed time series, are impossible. Westerberg *et al.* (2011) discussed some of the challenges related to calibration by traditional performance measures including the uncertainties in input and output data, variable sensitivity of performance measures with different flow magnitudes and temporal inconsistency of input and output data. To overcome the challenge, novel calibration measures without direct time series comparisons are instead used, such as synthetic regional flow duration curves (FDCs) (Yu & Yang 2000; Westerberg *et al.* 2011), the slope of FDCs (Yadav *et al.* 2007; Yilmaz *et al.* 2008), spectral properties (Montanari & Toth 2007), recession curves (Lamb & Beven 1997; Winsemius *et al.* 2009) and the base flow index (Bulygina *et al.* 2009).

The second challenge of regionalization, which transfers model parameter values from gauged to un-gauged or poorly gauged catchments (Blöschl & Sivapalan 1995; Parajka *et al.* 2005; Samaniego *et al.* 2011), becomes increasingly important. Regionalization methods can be classified into three categories: (1) multiple regression analysis method which relate model parameter values to some physical attributes of the catchments (Abdulla & Lettenmaier 1997; Seibert 1999; Xu 1999a, 2003; Fernandez *et al.* 2000; Kokkonen *et al.* 2003; Hundecha & Bárdossy 2004; Parajka *et al.* 2005; Bárdossy & Singh 2011); (2) spatial proximity methods by either adopting a calibrated parameter set from the nearest neighbour catchment (Burn & Boorman 1993; Huang *et al.* 2003) or interpolating calibrated parameters spatially (Parajka *et al.* 2005); and (3) catchment similarity methods which involve adopting a calibrated parameter set from the most physically similar catchment or interpolating calibrated parameters in similarity space (Xu 1999b; Jin *et al.* 2009). Kokkonen *et al.* (2003) concluded that, in hydrological research, it is better to adopt the entire set of calibrated parameters from the gauged basin instead of deriving quantitative relationships between basin characteristics and model parameters. The problem of estimating model parameters in un-gauged basins is a major issue which merits further investigation.

During the past two decades, numerous datasets have been developed for global/regional hydrological assessment and modelling. These datasets often show differences in their spatial and temporal distributions of precipitation, however, which is one of the most critical input variables in global/regional hydrological modelling. Many studies have therefore compared differences between the various precipitation datasets and rain gauge data as well as their impact on hydrological modelling (Fekete *et al.* 2004; Tian *et al.* 2007; Biemans *et al.* 2009; Abdella & Alfredsen 2010; Shen *et al.* 2010; Li *et al.* 2012). These precipitation datasets generally agree in their temporal trends and spatial distribution, but they often show remarkable differences at regional scales (Costa & Foley 1998; Oki *et al.* 1999; Adler *et al.* 2001). Fekete *et al.* (2004) compared six monthly precipitation datasets to assess their uncertainties and associated impacts on the terrestrial water balance. The study highlighted the need to improve precipitation estimates in arid and semiarid regions, where slight changes in precipitation can result in dramatic changes in the runoff response due to the non-linearity of the runoff-generation processes. Furthermore, seven global gridded precipitation datasets were compared at river basin scale in terms of annual mean and seasonal precipitation by Biemans *et al.* (2009). This study revealed that the representation of seasonality was similar for all the datasets but noted large uncertainties in the mean annual precipitation, especially in mountainous, arctic and small basins.

Large-scale global precipitation datasets that have been commonly used in previous studies include the Climate Research Unit (CRU; CRU 2000), the Tropical Rainfall Measuring Mission (TRMM; Huffman *et al.* 2007) and the Global Precipitation Climatology Project (GPCP; Huffman *et al.* 2001). Some studies have shown that satellite-based precipitation products can be used as an alternative source of information, but these need calibration and validation due to the indirect nature of the radiation measurements (Tobin & Bennett 2010; Cheema & Bastiaanssen 2012). New meteorological forcing data developed by the European Union funded Water and Global Change (WATCH) project (www.eu-watch.org), the WATCH Forcing Data (WFD), were made available for use from August 2011 (Weedon *et al.* 2010, 2011). This dataset was derived from the reanalysis of the European Centre for Medium-Range

Weather Forecasts (ERA40; Uppala *et al.* 2005) for the period 1958–2001, and was bias corrected based on monthly observational data (Mitchell & Jones 2005).

As is already known, satellite-based precipitation products such as TRMM have shorter periods starting from 1997 but are quite popular as they are updated regularly. The WFD on the other hand, with a longer bias-corrected record, is ideal for analysing the historical trends. Although some studies using the WFD have shown that it improves acceptable simulations of river runoff in some regions (Piani *et al.* 2010; Hagemann *et al.* 2011), its usefulness in many regions is yet to be analysed. Our literature survey shows that comparisons of the TRMM and the WFD in driving large-scale hydrological models in southern Africa have not yet been reported. This is particularly important because of the limited rain gauge data available for model calibration in the region.

From the foregoing concerns, it is clear that: (1) there is a need for systematic comparison of the consistency and difference between the satellite-based TRMM and the bias-corrected WFD datasets in terms of their spatio-temporal variation of precipitation in southern Africa; (2) there is a need to evaluate the performance of the two global datasets (TRMM and WFD) in driving large-scale hydrological models (e.g. WASMOD-D; Widen-Nilsson *et al.* 2009; Gong *et al.* 2011) at gauged basins; and (3) there is a need to compare water resources simulated by hydrological models using regionalization with the TRMM and WFD datasets. The above considerations form the basis of this study, which will be useful to the large-scale hydrology community by providing some insights into the selection and applicability of global weather datasets for research in other data-scarce regions.

STUDY AREA AND DATA

Study area

The region under study is continental southern Africa (latitude 9–35°S and longitude 10–41°E), which comprises Angola, Botswana, Lesotho, Malawi, Mozambique, Namibia, South Africa, Swaziland, Zambia and Zimbabwe (Figure 1). Although most of southern Africa is classified as semiarid to arid, the region has a wide range of contrasting hydro-meteorological conditions. The climate of southern Africa is complex due to its steep orography, contrasted oceanic surroundings and atmospheric dynamics (Fauchereau *et al.* 2003), which have resulted in a wide range of contrasting hydro-meteorological regions. Spatially, there is a marked east to west gradient of humid to arid conditions as well as north to south latitudinal rainfall variation. The southernmost parts (Botswana, Lesotho, Namibia, South Africa and Swaziland) experience lower rainfall than the northern parts (Angola, Malawi, Mozambique, Zambia and Northern Zimbabwe). Rainfall is strongly seasonal with over 80% of the annual total occurring during the austral summer months during November–April when the Inter-tropical Convergence Zone (ITZC) and the Congo Air Boundary (CAB), semi-permanent subtropical high-pressure systems located in the southwest Indian and southeast Atlantic Oceans respectively, are active in the region. The region is further characterized by high inter-annual rainfall variability, especially in the drier regions, as evidenced by the droughts of 1992, 1995 and 1998 and floods of 2000 and 2001 (Unganai & Kogan 1998; Bartman *et al.* 2003; Kandji *et al.* 2006; Layberry *et al.* 2006; Love *et al.* 2010; Ngongondo *et al.* 2011).

Major river basins in the region include the Limpopo, Orange, Okavango and Zambezi which are all transboundary and highly regulated at various points along their course for water supply and hydropower generation (Vörösmarty and Moore 1991; Turton *et al.* 2004; Zhu & Ringler 2010; Beck & Bernauer 2011).

Data

This study used HYDRO1 k (USGS 1996a) to delineate the basin boundaries. HYDRO1 k is derived from the GTOPO30 30-arc-second global-elevation dataset (USGS 1996b) and has a spatial resolution of 1 km. HYDRO1 k is hydrographically corrected such that local depressions are removed and basin boundaries are consistent with topographic maps.

Two precipitation datasets were used in the study. The first dataset was constructed by combining a 0.25 and a 1 degree dataset: the TRMM 3B42 dataset (Huffman *et al.* 2007) which covers latitudes 50°S–50°N, and the GPCP

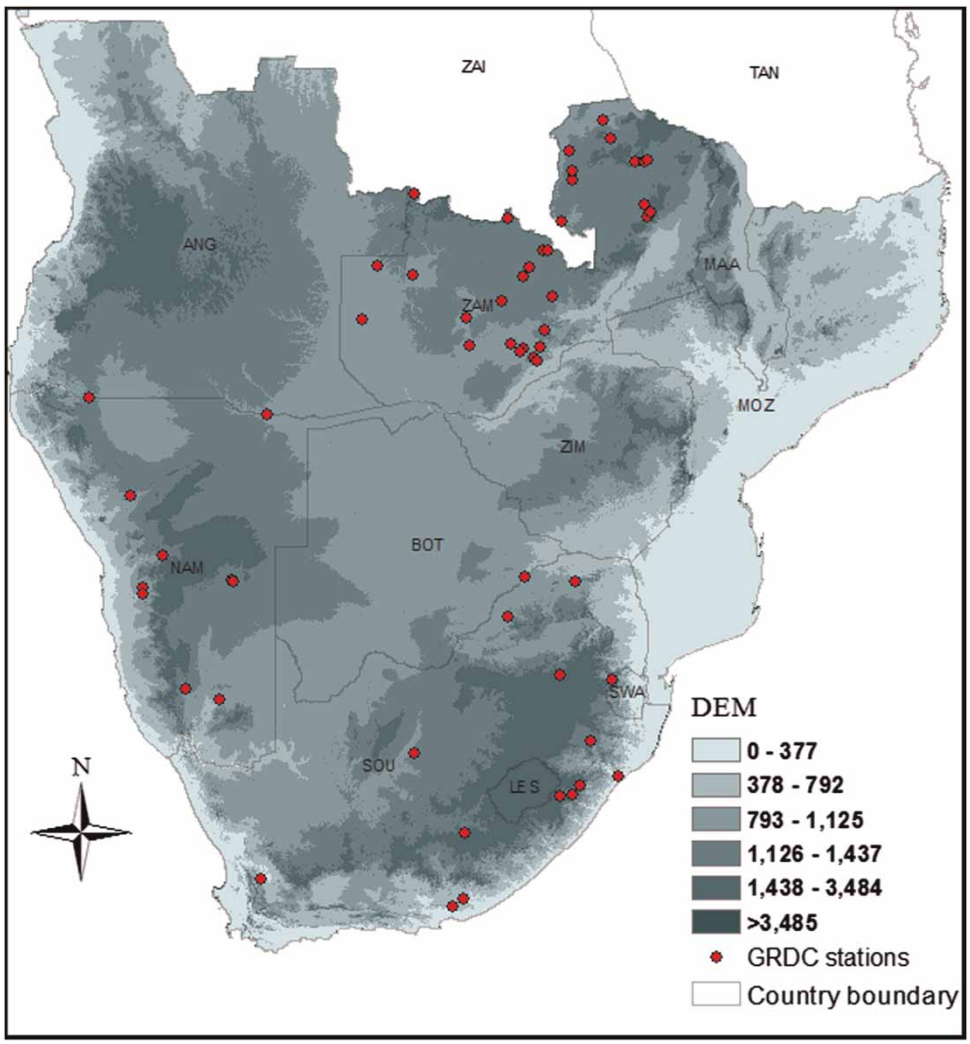

Figure 1 | Topographic map of southern Africa with Global Runoff Data Centre (GRDC) stations used in the study.

1DD dataset (Huffman *et al.* 2001) which covers the whole globe.

The objective of TRMM is to understand the distribution of tropical rainfall and its relation to the global water and energy cycles (Adler *et al.* 2007). TRMM datasets have been used to calibrate distributed hydrological models in large river basins (e.g. Collischonn *et al.* 2008; Su *et al.* 2008; Milzow *et al.* 2011; Li *et al.* 2012) as well as flood modelling (Harris *et al.* 2007). The TRMM project aims to provide small-scale variability of precipitation by frequent, closely spaced observations. TRMM uses a combination of microwave and infrared sensors to improve accuracy, coverage and resolution of its precipitation estimates; however, the ability of TRMM to specify moderate and light precipitation over short time intervals is poor. In common with the GPCP products, TRMM was designed to combine precipitation estimates from satellite instruments with land-surface gauges (Huffman *et al.* 2007). For instance, the TRMM 3B42 dataset was scaled to match the TRMM 3B43, a monthly dataset bias corrected and combined with rain gauge data. We rescaled the combined precipitation to 0.5 degree through linear interpolation.

The second precipitation dataset used in the study is the WFD developed by the WATCH project (Weedon *et al.* 2010, 2011) as inputs for large-scale land-surface and hydrological models. The WFD consists of meteorological variables needed to run hydrological models derived from ERA-40 reanalysis (Uppala *et al.* 2005), including 2 m air

temperature, wind speed, 10 m surface pressure and specific humidity, downward longwave and shortwave radiation, rainfall and snowfall rates. The ERA-40 data were bi-linearly interpolated to 0.5 degree using the land-sea mask from the CRU dataset TS2.1 (Mitchell & Jones 2005). The CRU dataset was also used to bias correct monthly temperature and number of wet days. The Global Precipitation and Climatology Centre (GPCC; Huffman *et al.* 2001) and rain gauges were used to bias correct monthly precipitation. Data including 2 m air temperature, minimum temperature and dew point temperature are used in this study for calculating daily potential evapotranspiration (Allen *et al.* 1998). In this study, WFD daily minimum temperature was computed by using WFD 3-hourly minimum temperature. Daily discharge time series for the test basins were taken from the Global Runoff Data Centre (GRDC) database (http://www.bafg.de/GRDC/EN/Home/homepage__node.html).

Data from 57 GRDC gauging stations (Figure 1) were obtained in the form of daily gauge heights and periodic discharge measurements for each station. After quality control for record length and completeness, unrealistic runoff coefficients, precipitation and discharge data consistency, etc., 22 discharge stations in southern Africa were retained for further analysis. The maximum overlapping period of the two global precipitation datasets (TRMM and WFD) used for calibration was 1996–2001. Table 1 lists the characteristics of the study basins in southern Africa.

METHODS

Statistical analysis

In order to compare the consistency and differences between the two global precipitation datasets, i.e. TRMM and WFD, several statistical and hypothesis testing methods have been used in this paper including: the Mann–Kendall (MK; Mann 1945; Kendall 1975; Zhang *et al.* 2008, 2009; Chu *et al.* 2010; Kumar & Jain 2011) method for testing whether the two datasets reveal the same changing trend; Kolmogorov–Smirnov (KS) test for checking whether the two datasets have the same distribution pattern (Xu 2001); and student's *t*-test and *F*-test for checking the equality of mean value and variance between the two global datasets, respectively. A 5% significance level was used for the above tests.

Mann–Kendall test

The MK test is used to analyse trends in the precipitation series across southern Africa. The steps of the MK method adopted in this study are as follows (Chu *et al.* 2010).

The first-order autocorrelation coefficient is calculated as:

$$\rho_1 = \frac{Cov(x_i, x_{i+1})}{\mathrm{var}(x_i)} = \frac{\frac{1}{n-2}\sum_{i=1}^{n-1}(x_i - \overline{x})(x_{i+1} - \overline{x})}{\frac{1}{n-1}\sum_{i=1}^{n}(x_i - \overline{x})^2} x_{i-1} \quad (1)$$

Second, remove the autocorrelation from the original time series if it is statistically significant:

$$x'_i = x_i - \rho_1 x_{i-1} \quad (2)$$

The Kendall indicator τ, variance σ_τ^2 and normalized variable U are calculated based on the transferred series x'_i as:

$$\tau = \frac{4p}{n(n-1)} \quad (3)$$

$$\sigma_\tau^2 = \frac{2(2n+5)}{9n(n-1)} \quad (4)$$

$$U = \tau/\sigma_\tau^2 \quad (5)$$

where p is the number of dual observations in the precipitation time series, i.e. the number of times that $x'_{t_2} > x'_{t_1}$ for all t_1, $t_2 = 1,\ldots, n$ such that $t_2 > t_1$. U reflects the trend in time series, of which the larger value means the more obvious trend. There is an increasing trend if U is larger than zero, and vice versa. At a significance level α, the hypothesis of no trend is rejected if:

$$|U| > U_{1-\alpha/2}$$

where $U_{1-\alpha/2}$ can be sourced from the standard normal distribution table.

Table 1 | Properties of the study basins in southern Africa

No.	Station name	River name	Country	Lat.	Long.	Area (km^2)
47	Elands Drift Aspoort	Doring	ZA	−32.50	19.54	6,903
56	Fp 1609030 The Banks	Mzimkulu	ZA	−29.78	29.47	545
70	Wolvekrans	Olifants	ZA	−26.01	29.25	3,256
77	Rundu	Okavango	NA	−17.90	19.75	97,300
160	Kaleni Hill Road Bridge	Zambezi	ZM	−11.13	24.25	764
166	Nyimba	Kafue	ZM	−15.75	27.30	1,36,234
168	Itezhi–Tezhi	Kafue	ZM	−15.77	26.02	96,239
170	Machiya	Kafue	ZM	−14.42	27.00	23,065
174	Kaleya Dam Site	Magoye	ZM	−16.25	28.13	1,865
176	Chimbumbu Farm	Luswishi	ZM	−15.97	27.60	2,668
178	Ndubeni	Kafue	ZM	−13.40	27.82	18,509
180	Wusakili	Kafue	ZM	−12.88	28.25	9,088
182	Baluba	Baluba	ZM	−12.87	28.37	339
183	Great North Road Bridge	Mulungushi	ZM	−14.30	28.55	1,448
185	Kalabo	Luanginga	ZM	−14.97	22.68	34,621
187	Chipili	Lufubu (Trib. Luapula)	ZM	−10.72	29.08	1,220
189	Kapuma Falls	Mutotoshi	ZM	−9.48	30.23	383
190	Nsama	Mwambeshi	ZM	−8.90	29.97	707
191	Ntumbachushi Falls	Ngona	ZM	−9.85	28.95	303
192	Mpika/Kasama Road Bridge	Kanchibiariver	ZM	−11.50	31.28	1,215
193	Kasama/Luwingu Road Bridge	Lukulu	ZM	−10.18	30.97	6,504
194	Mpika Road Bridge	Lwitika	ZM	−11.83	31.38	324

Kolmogorov–Smirnov test

The KS test is used to determine whether the distribution of the data is the same or different from the predetermined distribution and to test the significance of the similarity or dissimilarity (Xu 2001). The KS test is conducted as follows.

1. Calculate the expected cumulative frequency (values of cumulative distribution function) $F^e(x)$.
2. Calculate the sample cumulative frequency, $F^e(x) = k/n$, where k is the number of observations less than or equal to x and n is the total number of observations.
3. Determine the maximum deviation $D = \max/F^e(x) - F^o(x)$
4. If the value D is greater than or equal to the critical tabulated value of the KS statistic for the chosen significance level, the hypothesis that the data fit the tested distributed is rejected.

Student's *t*-test and *F*-test

The student's t-test is used to assess whether the means of two samples are statistically different from each other. Under the null-hypothesis of equal sample means (H_0:$\mu_1 = \mu_2$) and alternate hypothesis of unequal sample means (H_0:$\mu_1 \neq \mu_2$), the t-statistic is calculated as:

$$t = \frac{(\bar{x}_1 - \bar{x}_2)}{\sqrt{s_1^2/n_1 + s_2^2/n_2}} \tag{6}$$

The null hypothesis H_0 is rejected if:

$$|t| = \frac{\left(t_{1-\alpha/2,n_1-1} \cdot s_1^2/n_1 + t_{1-\alpha/2,n_2-1} \cdot s_2^2/n_2\right)}{s_1^2/n_1 + s_2^2/n_2} \tag{7}$$

where $\bar{x}_1$ and $\bar{x}_2$ are sample means; s_1^2 and s_2^2 are the sample variances; and n_1 and n_2 are sample sizes. The values of $t_{1-\alpha/2,n_1-1}$ and $t_{1-\alpha/2,n_2-1}$ can be sourced from student's t-distribution table.

The F-test is used to determine whether two sample variances are different. Under the null hypothesis of equal variances $(H_0{:}\sigma_1^2 = \sigma_2^2)$ and the alternate hypothesis of unequal variances $(H_0{:}\sigma_1^2 \neq \sigma_2^2)$, the F-statistic is calculated as:

$$F_c = s_1^2/s_2^2 \quad s_1^2 > s_2^2 \tag{8}$$

The null hypothesis H_0 is rejected if:

$$F_e = F_{1-\alpha,n_1-1,n_2-1}, \tag{9}$$

where the critical value of $F_{1-\alpha,n_1-1,n_2-1}$ can be sourced from the F-distribution table.

WASMOD-D

The water and snow balance modelling system at the macro scale (WASMOD-D; Widen-Nilsson *et al.* 2009; Gong *et al.* 2011), developed based on WASMOD (Xu *et al.* 1996; Xu 2002), was used in the study. The input data included daily values of precipitation, temperature and potential evapotranspiration. The daily WASMOD-D calculates snow accumulation and melt and actual evapotranspiration, and separates runoff into fast flow and slow flow. Potential evapotranspiration is defined as follows:

$$ep_t = E_c\left(T_a^+\right)^2(100 - \mathrm{RH}) \tag{10}$$

where ep_t is potential evapotranspiration (mm day^{-1}); T_a is the daily air temperature (°C); E_c was set to 0.018/30 (mm day^{-1} °C^{-2}); and RH (%) is relative humidity calculated from air temperature and dew point temperature.

Snow accumulation and melt are derived from:

$$sn_t = p_t\left\{1 - \exp\left[-\left(\frac{T_a - a_1}{a_1 - a_2}\right)^2\right]\right\}^+ \tag{11}$$

$$sp_t = sp_{t-1} + sn_t - m_t \tag{12}$$

$$m_t = sp_{t-1}\left\{1 - \exp\left[-\left(\frac{T_a - a_2}{a_1 - a_2}\right)^2\right]\right\}^+ \tag{13}$$

where sn_t is snowfall (mm day^{-1}); p_t is precipitation (mm day^{-1}); sp_t is snow storage (mm); m_t is snow melt (mm); parameters a_1 and a_2 are the snowfall temperature (°C) and snow melt temperature (°C). $(x)+$ means max$(x, 0)$.

Rainfall r_t (mm day^{-1}) is calculated via:

$$r_t = p_t - sn_t \tag{14}$$

Actual evapotranspiration e_t (mm day^{-1}) is calculated via:

$$e_t = \min\left[ep_t\left(1 - a_4^{w_t/ep_t}\right), w_t\right] \tag{15}$$

$$w_t = r_t + sm_{t-1}^+ \tag{16}$$

where ep_t is potential evapotranspiration (mm day^{-1}); w_t is available water (mm day^{-1}); sm_{t-1} is the land moisture (available storage); a_4 is a parameter (dimensionless).

Slow and fast flows are derived from equations as:

$$spa_t = 1 - e^{-c_1 w_t} \tag{17}$$

$$f_t = (r_t + m_t) \cdot spa_t \tag{18}$$

$$s_t = w_t(1 - e^{-c_2 w_t}) \tag{19}$$

$$d_t = s_t + f_t \tag{20}$$

where spa_t is saturated percentage area (%); s_t is slow flow (mm day^{-1}); f_t is fast flow (mm day^{-1}); d_t is total flow (mm day^{-1}); c_1 (mm^{-1}) and c_2 (mm^{-1}) are the parameters.

Finally, the water balance is achieved by updating land moisture:

$$sm_t = sm_{t-1} + r_t + m_t - e_t - d_t \tag{21}$$

where sm_t and sm_{t-1} are the land moisture at current and previous days (mm day^{-1}).

The aggregated network-response-function (NRF) routing algorithm developed by Gong *et al.* (2009) was used in this study for routing the runoff calculated by WASMOD-D. The NRF method preserves the spatially distributed time-delay information in the 1 km HYDRO1 k flow network in the form of simple cell-response functions for low-resolution grid (0.5°), where runoff is generated. Furthermore, the snow module was not considered in this study since there is rarely any snow even in winter in the mountainous areas of southern Africa. The version of WASMOD-D used in this study has only three parameters to be estimated: the actual evapotranspiration parameter a_4, the fast-runoff parameter c_1 and the slow-runoff parameter c_2. The time period used for this study was 1996–2001 and the first year (1996) was set aside as the spin-up period.

Model calibration

Calibration was made independently for each basin by searching for an 'optimal' parameter set at each discharge station used in southern Africa. In total, 5,000 parameter sets were obtained by Latin-Hypercube sampling (McKay *et al.* 1979) with prior uniform distribution from initial parameter-value ranges (Xu 2002; Gong *et al.* 2011). WASMOD-D was run with the 5,000 parameter sets and the resulting 5,000 runoff-generation time series were used as input to the routing model. At each grid resolution ($0.5^\circ \times 0.5^\circ$), 5,000 runoff time series were obtained from the WASMOD-D runs with the previously defined 5,000 parameter-value sets. The wave velocity that gave the highest efficiency was chosen for each resolution (Gong *et al.* 2009).

Potential evapotranspiration was calculated by the FAO-56 recommended Penman–Monteith equations (Allen *et al.* 1998). Runoff-generation parameters were then calibrated with the efficiency criteria, including the NS coefficient (Nash & Sutcliffe 1970), absolute value of the volume error (%) (VE; Widen-Nilsson *et al.* 2009) and the performance measure of FDC based on evaluation points (EPs) by using equal interval of flows ($R_{FDC,Q}$; Westerberg *et al.* 2011).

The FDC shows the percentage of time that a given flow rate is equalled or exceeded, which is constructed from flow data of a fixed time period (e.g. daily in this study). First, the flow data are sorted in order of decreasing flow. A unique ranking number i is assigned to each flow, starting with 1 for the maximum flow to n for the minimum flow, where n is the number of flow measurements. The probability P that a given flow will be equalled or exceeded is then defined by:

$$P_i(Q > Q_i) = (i - 0.5)/n \tag{22}$$

$$R_{\mathrm{FDC,Q}} = \sqrt{\sum_{i=1}^{k} \left(p_{sim,i} - p_{obs,i}\right)^2 / k} \tag{23}$$

where $P_i(Q \geq Q_i)$ is the exceedance probability of discharge Q_i which is the selected EPs by using equal interval of flows (Westerberg *et al.* 2011).

Here $k = 20$ was used, resulting in 19 EPs. The similarity of the FDCs for the observed and simulated flow series was evaluated using Equation (23), in which we can see that $R_{\mathrm{FEC,Q}}$ has a zero low bound; the closer the value to zero, the better the performance.

Regionalization method

To compare the results simulated by the two global precipitation datasets (TRMM and WFD) in un-gauged basins and in the whole studied region, regionalization of parameters in the southern Africa region was carried out. As discussed in the introduction section, many regionalization methods are described in the literature. The global mean method (Jin *et al.* 2009) was used in this study because of the small number of study basins, which meant that detailed assessments of parameter and catchment characteristics was unlikely to be robust and could probably mislead the results. The global mean method considers that the physical attributes of a catchment are represented by parameters and the average attributes over the region are represented by mean parameters.

RESULTS

Comparison of two precipitation datasets

Precipitation is the immediate source of water for the land-surface hydrological budget, and its uncertainty will strongly

impact the model calibration results. Figure 2 shows the difference in annual precipitation between the TRMM and the WFD datasets in 1997 (for illustrative purposes), while the mean annual precipitation difference between the TRMM dataset and the WFD dataset from 1997 to 2001 is shown in Figure 3. From these two figures, the following points are clear.

1. We can see that in general the spatial distributions of annual precipitation from two datasets are similar for both 1997 and mean annual (1997–2001). Mean annual precipitation in the region ranges from 0 to 400 mm yr^{-1} in the southwest to over 1,500 mm yr^{-1} in the north and the east.
2. We can also see that the mean annual precipitation difference between TRMM and WFD datasets is around ± 100 mm yr^{-1} in the extreme southern part of the region whereas the differences are larger in the north (± 100–500 mm yr^{-1}) and varies with geographic locations.
3. The difference between the two datasets has a clear geographic pattern, i.e. the precipitation derived from TRMM is considerably smaller than the WFD in the northwest the region, especially closer to Gabon and Congo, whereas in most parts in the central and the

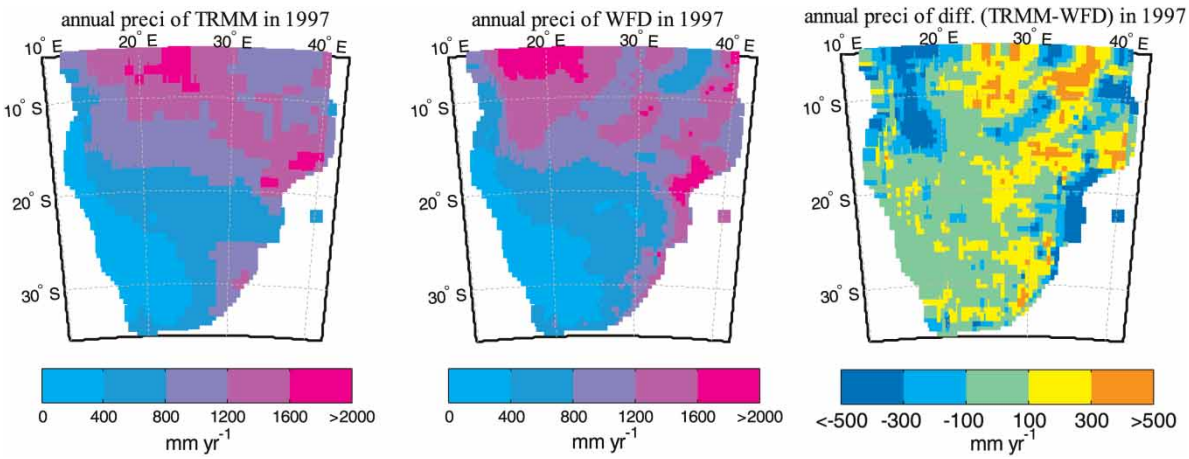

Figure 2 | Comparison of spatial distribution of annual precipitation in southern Africa from TRMM and WFD datasets in 1997.

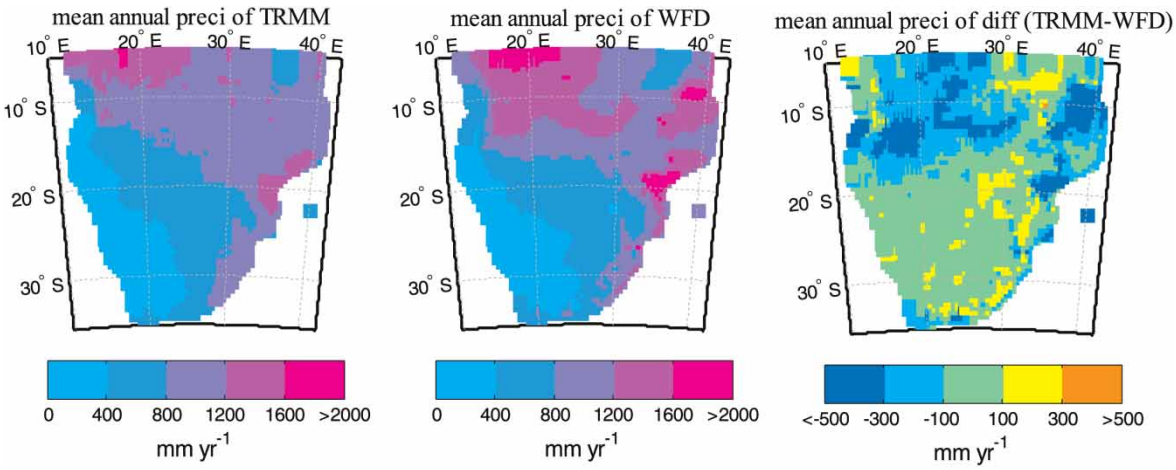

Figure 3 | Comparison of spatial distribution of mean annual precipitation in southern Africa from TRMM and WFD datasets (1997–2001).

south of the region the difference is small and it seems that the precipitation derived from TRMM is slightly larger than that from WFD.

4. The total precipitation derived from TRMM is less than that from WFD, which can be graphically confirmed by Figure 4 which shows a quantitative comparison of the spatial average of the mean monthly precipitation over southern Africa from TRMM and WFD during 1997–2001. Furthermore, it is seen that the monthly precipitation values of WFD are larger than those of TRMM in the wet period (November–April) and are slightly less in the dry period (May–October).

The results of the MK trend test for the two global precipitation datasets are shown in Figure 5 and Table 2. Figure 5 indicates that the spatial distribution of the temporal trends of daily precipitation derived from TRMM and WFD in southern Africa from 1997 to 2001 is similar

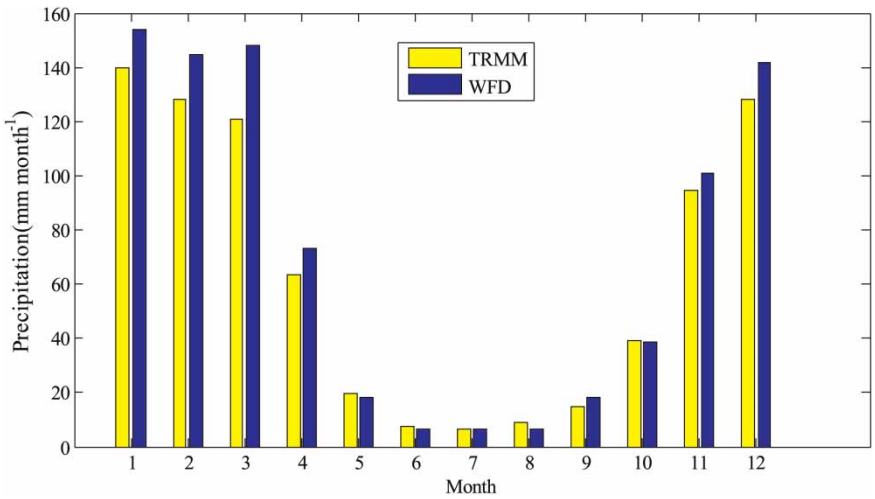

Figure 4 | Mean monthly precipitation in southern Africa from TRMM and WFD (1997–2001).

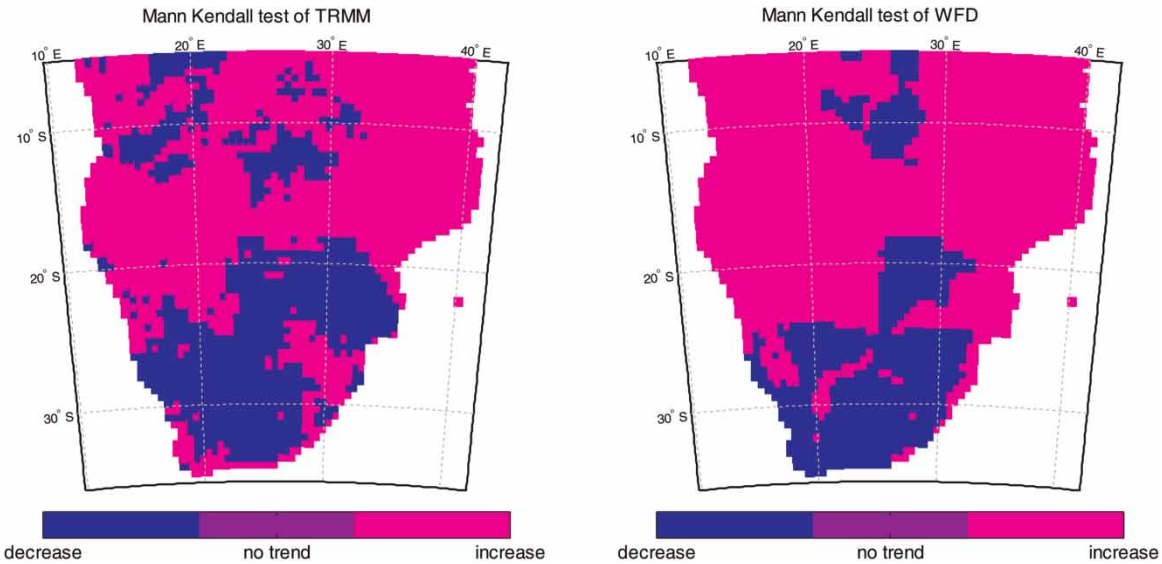

Figure 5 | Comparison of spatial distribution of MK temporal trend for daily precipitation from TRMM and WFD datasets in southern Africa (1997–2001).

Table 2 | The results of hypothesis test between TRRM and WFD in southern Africa

Total grid number = 2,635	Hypothesis	Number of grids
Kolmogorov–Smirnov test	The same distribution	191
	Not the same distribution	2,444
Mann–Kendall Test for TRMM	Decrease trend	973
	No trend	0
	Increase trend	1,662
Mann–Kendall Test for WFD	Decrease trend	726
	No trend	0
	Increase trend	1,909
Student's *t*-test	The same mean	1,534
	Not the same mean	1,101
F-test	The same variances	431
	Not the same variances	2,204

in general. In both cases, decreasing MK trends dominate in the south whereas increasing MK trends are dominant in the north of the region.

The results of the consistency test of the two global precipitation datasets in terms of their distribution patterns (KS test), long-term mean values (*t*-test) and variances (*F*-test) are shown in Figure 6 and Table 2. It is seen from Figure 6(a) that the hypothesis of the data belonging to the same distribution is rejected at 5% significance level in most parts of the region. Figure 6(b) indicates that, in the southern part of the region, long-term mean values of the two datasets are statistically equal at 5% significance level; this is not the case in large parts of the north. From Figure 6(c), we can see that the assumption that the variances of TRMM and WFD data are equal is rejected at 5% significance level in the majority of the region. These results are also summarized in Table 2, which presents the number of grids that reject or accept the null hypotheses of all the statistical tests applied in southern Africa.

Model performance

Statistical comparisons were carried out to evaluate the modelling results for the 22 selected gauged basins based on TRMM and WFD datasets. Table 3 shows the NS values and their associated VE and $R_{FDC,Q}$ values. For the TRMM dataset, the highest NS was 0.76 for the Kafue River basin at Machiya station and 20 basins had NS values larger than 0.5. For the WFD dataset, the highest NS was 0.94 for the Baluba basin and 17 basins had NS values larger than 0.5. The values of VE are mostly less than 10% for the two datasets. In general, the NS values derived from WFD were slightly higher than those from TRMM. In terms of the VE, the difference between the two datasets is very small.

Another important requirement of a hydrological model is the correct representation of the flow frequency. In this study, flow frequency is represented using a FDC which provides the percentage of time (duration) flow is exceeded over a historical period. The FDCs for six randomly selected basins are shown in Figure 7. There was a reasonably

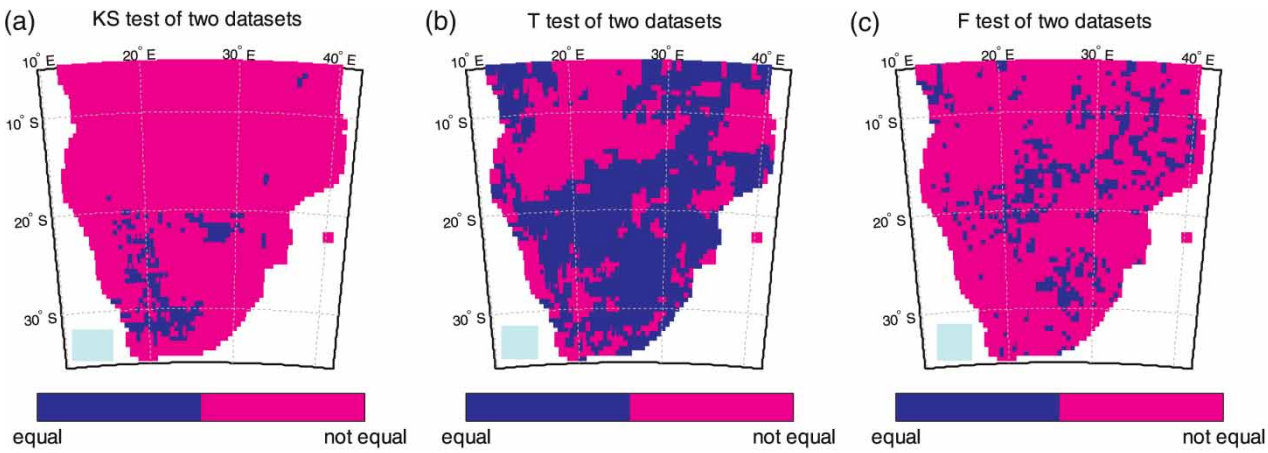

Figure 6 | Comparison of spatial distribution of general pattern by (a) KS test, (b) mean by student *t*-test and (c) variance by *F*-test of daily precipitation from TRMM and WFD datasets in southern Africa (1997–2001).

Table 3 | The indices of maximum NS and associated VE and $R_{FDC,Q}$ for all study basins in southern Africa

Station name	Country	Area (km^2)	WFD (1997–2001)			TRMM (1997–2001)		
			NS	VE (%)	$R_{FDC,Q}$	NS	VE (%)	$R_{FDC,Q}$
Elands Drift Aspoort	ZA	6,903	0.53	−9.84	0.67	0.32	−2.07	1.12
Fp 1609030 The Banks	ZA	545	0.55	0.57	1.46	0.49	5.47	1.42
Wolvekrans	ZA	3,256	0.53	−9.30	0.10	0.28	−17.22	0.15
Rundu	NA	97,300	0.67	4.35	0.08	0.59	2.56	0.06
Kaleni Hill Road Bridge	ZM	764	0.60	20.83	0.45	0.44	28.67	0.55
Nyimba	ZM	136,234	0.56	−1.78	0.23	0.44	−1.50	0.34
Itezhi–Tezhi	ZM	96,239	0.54	−14.35	0.19	0.55	−10.17	0.08
Machiya	ZM	23,065	0.83	−1.96	0.11	0.76	−20.61	0.09
Kaleya Dam Site	ZM	1,865	0.50	−12.06	0.11	0.61	−7.61	0.11
Chimbumbu Farm	ZM	2,668	0.78	−3.32	0.36	0.67	−5.75	0.48
Ndubeni	ZM	18,509	0.87	−2.44	0.13	0.73	−9.42	0.12
Wusakili	ZM	9,088	0.63	−3.51	0.14	0.56	0.00	0.10
Baluba	ZM	339	0.94	−2.66	0.14	0.56	1.30	0.37
Great North Road Bridge	ZM	1,448	0.64	−12.95	0.50	0.65	−7.59	0.40
Kalabo	ZM	34,621	0.87	0.00	0.02	0.74	−1.85	0.01
Chipili	ZM	1,220	0.36	−4.67	1.96	0.63	5.04	1.10
Kapuma Falls	ZM	383	0.57	1.31	0.11	0.62	3.40	0.13
Nsama	ZM	707	0.58	2.46	0.60	0.59	−7.31	0.25
Ntumbachushi Falls	ZM	303	0.71	2.89	0.13	0.69	−1.01	0.09
Mpika/Kasama Road Bridge	ZM	1,215	0.22	−1.00	0.28	0.69	−4.12	0.23
Kasama/Luwingu Road Bridge	ZM	6,504	0.65	4.79	0.34	0.50	3.93	0.44
Mpika Road Bridge	ZM	324	0.69	1.44	0.30	0.73	0.96	0.27

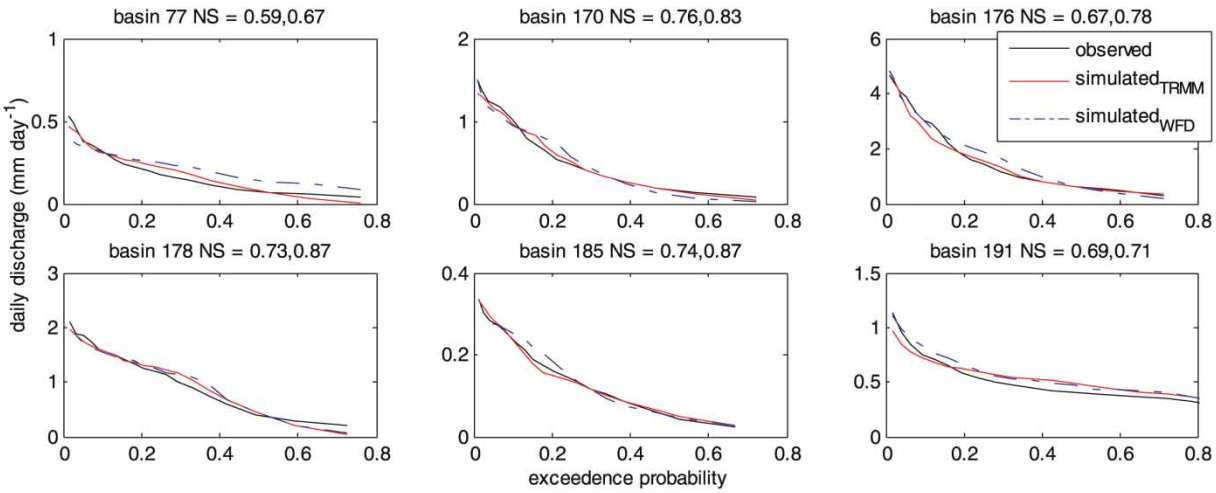

Figure 7 | FDCs of six basins in southern Africa based on TRMM and WFD datasets for daily discharge simulations from 1997 to 2001 (notice the scale difference in *y* axis. Basin numbers are listed in Table 1. NS = NS of TRMM, NS of WFD.

Table 4 | Comparison of FDCs (observed) for six basins in southern Africa with TRMM and WFD datasets from 1997 to 2001 with exceeding probability equal to 5, 50 and 95% (mm day^{-1})

Exceeding probability	5%			50%			95%		
Basin number	Observed	TRMM	WFD	Observed	TRMM	WFD	Observed	TRMM	WFD
No.191	0.933	0.832	0.960	0.397	0.469	0.459	0.112	0.193	0.117
No.185	0.285	0.287	0.277	0.056	0.064	0.038	0	0	0
No.178	1.851	1.769	1.776	0.444	0.499	0.520	0.359	0	0
No.176	3.855	3.687	3.818	0.625	0.736	0.753	0	0	0
No.170	1.227	1.170	1.181	0.181	0.153	0.121	0	0	0.120
No.77	0.418	0.395	0.352	0.086	0.091	0.151	0	0	0.039

close match between the observed and simulated FDCs for both datasets. A quantitative comparison is provided in Table 4, which shows the observed and simulated runoff of the six basins based on the TRMM and WFD datasets from 1997 to 2001 for exceedance probabilities $P = 5$, 50 and 95%. It indicates that: (1) the runoff derived from the WFD is closer to the observed runoff than those from the TRMM, especially for high flows with $P = 5\%$; (2) for the median flows when the $P = 50\%$, the runoff derived from the TRMM is slightly closer to the observed than that from WFD; (3) for the high flows, the simulated runoff based on TRMM and WFD all underestimated the observed flows whereas the median flows are slightly overestimated; and (4) all runoffs (simulated and observed) are nearly zero when $P \geq 95\%$.

Regional water resources assessment by global mean method

The regionalization method was based on the transfer of locally calibrated parameter sets to un-gauged basins using the arithmetic global mean estimation method for both datasets. The mean values of parameters a_4, c_1 and c_2 are 0.97, 1.84×10^{-4} and 0.81×10^{-5} from WFD, while they are 0.817, 1.38×10^{-4} and 0.35×10^{-5} from TRMM. The average annual runoff in southern Africa simulated with WASMOD-D based on TRMM is 96.47 mm yr^{-1}, which is larger than that based on WFD of 80.89 mm yr^{-1}. The average annual actual evapotranspiration from TRMM is 682.72 mm yr^{-1} and is 782.92 mm yr^{-1} from WFD. We can therefore see that the absolute annual water balance errors based on TRMM and WFD datasets (which equals average annual precipitation less average annual runoff less average annual actual evapotranspiration) are -8 and 6 mm yr^{-1}, respectively.

Details of the spatial distribution of the mean annual runoff and actual evapotranspiration simulated by WASMOD-D using the two global precipitation datasets from 1997 to 2001 are depicted in Figure 8. It is seen that: (1) in general, the average annual runoff from TRMM is larger than those from WFD, especially in northwest of the region; (2) the distribution of the annual actual evapotranspiration from the two datasets is quite similar in most areas, except in the northwest part where the WFD dataset results in higher evapotranspiration values; and (3) both datasets give more or less consistent results in the wetter parts of southern Africa covering the east of Angola, Zambia, Malawi, Mozambique and the eastern coastline of South Africa.

Furthermore, the spatial distribution of the mean annual runoff across southern Africa simulated in this study agrees well with the distribution patterns produced by Bullock *et al.* (1997) for the period of 1961–1990. The spatial distributions of the simulated monthly mean runoff (1997–2001) for the wet season (November–April) and the dry season (May–October) in southern Africa based on TRMM and WFD datasets are depicted in Figure 9. It indicates that the northern and eastern parts of the region have more available water resources while the southwest part is quite dry around the year. Most of the southwest part is actually a hot desert covering large parts of Botswana and Namibia. In addition, the spatial distribution of simulated monthly mean runoff based on the two global precipitation datasets has a similar pattern. However, the simulated monthly mean runoff derived from the TRMM dataset is larger than that from WFD.

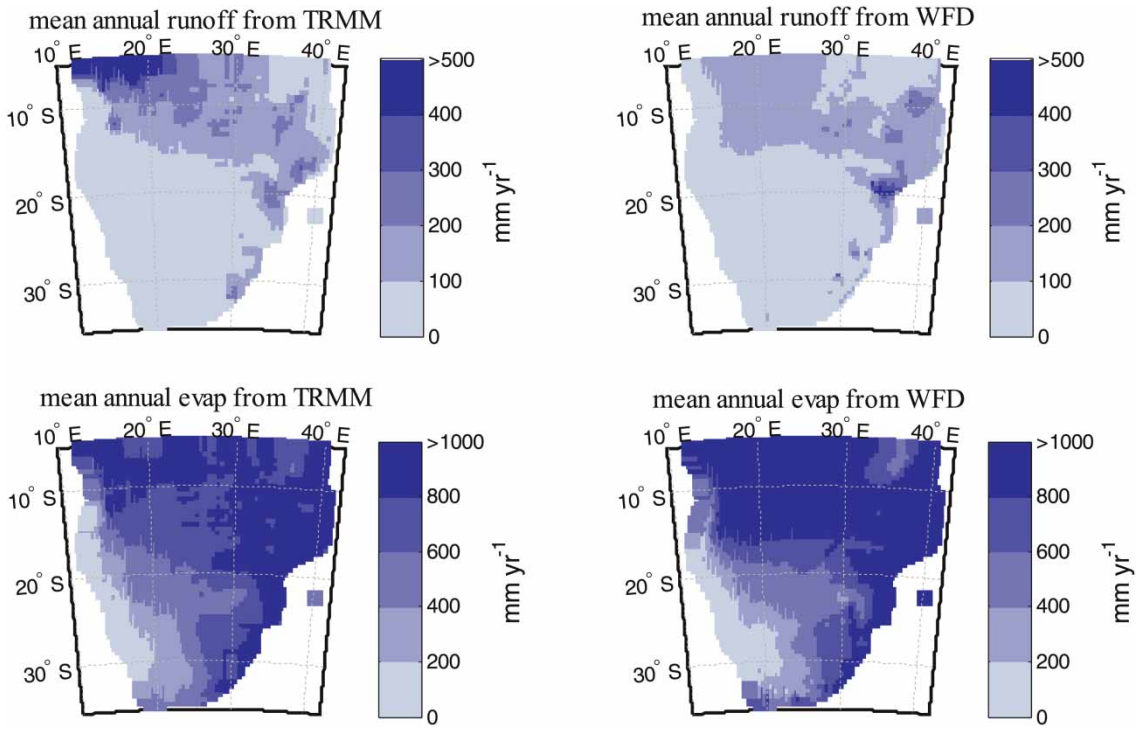

Figure 8 | Spatial distribution of mean annual (1997–2001) runoff and evapotranspiration in southern Africa simulated using WASMOD-M from TRMM and WFD datasets.

CONCLUSIONS

In this study, the spatio-temporal variations of precipitation in southern Africa based on the two global precipitation datasets, the TRMM and WFD, have been compared by using four statistical testing methods (MK test, KS test, the student's *t*-test and the *F*-test). The two global precipitation datasets are then used as inputs to the WASMOD-D model to simulate water balance components of 22 gauged catchments in the region and the consistency and differences of the simulation results are compared. The arithmetic global mean regionalization approach is used to obtain regional parameter values and the water balance components for southern Africa are then simulated with the two global precipitation datasets as input to the model. The results of the simulations are evaluated by the NS coefficient, the absolute value of the VE (%), the performance measure of FDC based on EPs by using equal interval of flows ($R_{FDC,Q}$) and visual inspection of the FDCs.

The following conclusions can be drawn from the results of this study.

1. The regional spatial distribution of the mean annual precipitation and the temporal trend from TRMM and WFD datasets is comparable. However, remarkable differences exist in monthly and annual mean values and in the variances. The TRMM annual total precipitation is in general less than the WFD annual total precipitation. There are however larger differences between the two datasets in terms of their variances than in their mean values and spatial patterns.
2. Regional application of the WASMOD-D based on the two datasets produced results with model performances of above 0.5 for the NS coefficient, below 10% for the VE and a good reproduction of the observed FDCs for the majority of the basins. However, NS coefficient values lower than 0.5 and absolute value of the VE larger than 20% are also found in a few basins, which agrees with the literature reports of global hydrological modelling studies.
3. The simulated regional average annual runoff based on the two datasets is 96.47 and 80.89 mm yr^{-1} respectively. The regionalization results indicate that the application

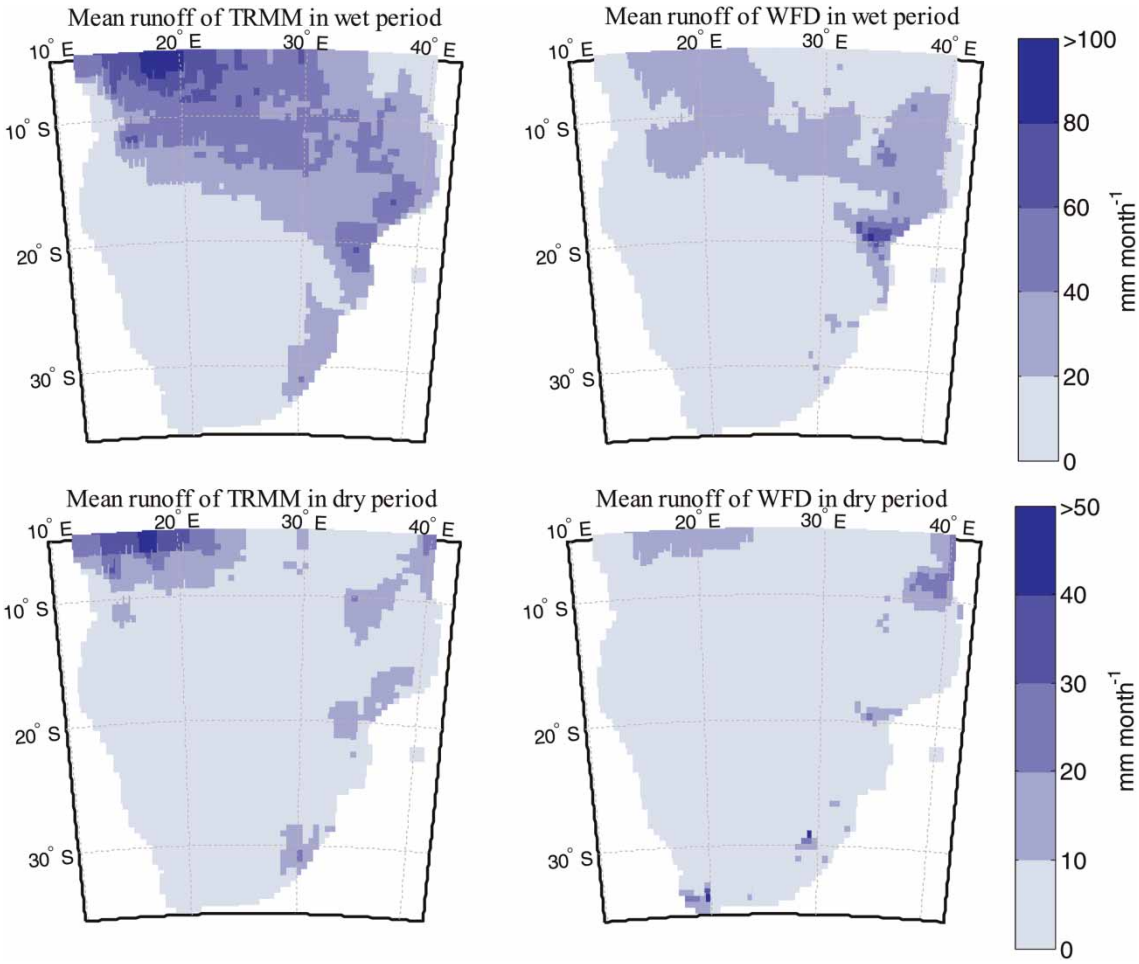

Figure 9 | Spatial distribution of mean monthly (1997–2001) runoff in wet period (November–April) and dry period (May–October) in southern Africa simulated using WASMOD-D from TRMM and WFD datasets (note the difference in legends).

of WASMOD-D based on the WFD results in slightly better performance than that based on TRMM.

4. The moderate performance level of the model simulations from the gauged catchments in the region and the regionalization is indicative that limitations in data quality and quantity can seriously constrain any efforts in large-scale modelling. The collection of additional data in southern Africa would therefore be very helpful in further regional water resources assessments.

ACKNOWLEDGEMENTS

We are grateful to Dr Graham Weedon within the WATCH project group for providing the free global data we used. This study was jointly funded by the Norwegian Research Council (RCN) Environment and Development Programme (FRIMUF) project number 171783 and project 190159/V10 (SoCoCA), and the project on capacity building in water sciences for the better management of water resources in southern Africa (NUFUPRO-2007) funded by the Norwegian Programme for Development, Research and Education (NUFU).

REFERENCES

Abdella, Y. & Alfredsen, K. 2010 Long-term evaluation of gauge-adjusted precipitation estimates from a radar in Norway. *Hydrology Research* **41** (3–4), 171–192.

Abdulla, F. A. & Lettenmaier, D. P. 1997 Development of regional parameter estimation equations for a macroscale hydrologic model. *Journal of Hydrology* **197** (1–4), 230–257.

Adeloye, A. J. & Rustum, R. 2012 Self-organising map rainfall-runoff multivariate modelling for runoff reconstruction in inadequately gauged basins. *Hydrology Research* **43** (5), 603–617.

Adler, R., Braun, S., Stocker, E. & Marius, J. 2007 Tropical Rainfall Measuring Mission, TRMM, Senior Review Proposal, Tech. rep., Laboratory for Atmospheres, NASA Goddard Space Flight Centre, Greenbelt, Maryland, USA, p. 9125.

Adler, R. F., Kidd, C., Petty, G., Morissey, M. & Goodman, H. M. 2001 Intercomparison of Global Precipitation Products: The Third Precipitation Intercomparison Project (PIP-3). *Bulletin of the American Meteorological Society* **82** (7), 1377–1396.

Allen, R. G., Pereira, L. S., Raes, D. & Smith, M. 1998 *Crop Evapotranspiration: Guidelines for Computing Crop Water Requirements-FAO Irrigation and Drainage Paper 56*. FAO, Rome, 300, p. 6541.

Arheimer, B., Dahné, J., Donnelly, C., Lindström, G. & Strömqvist, J. 2012 Water and nutrient simulations using the HYPE model for Sweden vs. the Baltic Sea basin – influence of input-data quality and scale. *Hydrology Research* **43** (4), 315–329.

Arnell, N. W. 1999 Climate change and global water resources. *Global Environmental Change* **9**, S31–S49.

Arnell, N. W. 2004 Climate change and global water resources: SRES emissions and socio-economic scenarios. *Global Environmental Change* **14** (1), 31–52.

Bárdossy, A. & Singh, S. K. 2011 Regionalization of hydrological model parameters using data depth. *Hydrology Research* **42** (5), 356–371.

Bartman, A. G., Landman, W. A., De, W. & Rautenbach, C. J. W. 2003 Recalibration of General Circulation Model output to austral summer rainfall over southern Africa. *International Journal of Climatology* **23** (12), 1407–1419.

Beck, L. & Bernauer, T. 2011 How will combined changes in water demand and climate affect water availability in the Zambezi River basin? *Global Environmental Change* **21** (3), 1061–1072.

Beven, K. J. & Freer, J. 2001 Equifinality, data assimilation, and uncertainty estimation in mechanistic modelling of complex environmental systems using the GLUE methodology. *Journal of Hydrology* **249** (1–4), 11–29.

Biemans, H., Hutjes, R. W. A., Kabat, P., Strengers, B. J., Gerten, D. & Rost, S. 2009 Effects of precipitation uncertainty on discharge calculations for main river basins. *Journal of Hydrometeorology* **10** (4), 1011–1025.

Blöschl, G. & Sivapalan, M. 1995 Scale issues in hydrological modelling: a review. *Hydrological Processes* **9** (3–4), 251–290.

Bullock, A., Andrews, A. J., Mkhandi, S., Mngodo, R. & Hughes, D. A. 1997 *Southern African FRIEND. International Collaboration in the Hydrological Science of Flow Regime. Sustainability of Water Resources under Increasing Uncertainty*. IAHS Press, Institute of Hydrology, Wallingford, Oxfordshire, p. 133.

Bulygina, N., McIntyre, N. & Wheater, H. 2009 Conditioning rainfall-runoff model parameters for ungauged catchments and land management impacts analysis. *Hydrology and Earth System Sciences* **13** (6), 893–904.

Burn, D. H. & Boorman, D. B. 1993 Estimation of hydrological parameters at ungauged catchments. *Journal of Hydrology* **143** (3–4), 429–454.

Cheema, M. J. M. & Bastiaanssen, W. G. M. 2012 Local calibration of remotely sensed rainfall from the TRMM satellite for different periods and spatial scales in the Indus Basin. *International Journal of Remote Sensing* **33** (8), 2603–2627.

Chu, J., Xia, J., Xu, C., Li, L. & Wang, Z. 2010 Spatial and temporal variability of daily precipitation in Haihe River basin 1958–2007. *Journal of Geographical Sciences* **20** (2), 248–260.

Collischonn, B., Collischonn, W. & Tucci, C. E. M. 2008 Daily hydrological modeling in the Amazon basin using TRMM rainfall estimates. *Journal of Hydrology* **360** (1–4), 207–216.

Costa, M. H. & Foley, J. A. 1998 A comparison of precipitation datasets for the Amazon Basin. *Geophysical Research Letters* **25** (2), 155–158.

CRU 2000 *Climate Research Unit*, University of East Anglia. Available from: http://www.cru.uea.ac.uk (accessed September 2012).

Doll, P., Kaspar, F. & Lehner, B. 2003 A global hydrological model for deriving water availability indicators: model tuning and validation. *Journal of Hydrology* **270** (1–2), 105–134.

Fauchereau, N., Trzaska, S., Rouault, M. & Richard, Y. 2003 Rainfall variability and changes in southern Africa during the 20th century in the global warming. *Natural Hazards* **29**, 139–154.

Fekete, B. M., Vörösmarty, C. J. & Grabs, W. 2002 High-resolution fields of global runoff combining observed river discharge and simulated water balances. *Global Biogeochemical Cycles* **16** (3), 1042.

Fekete, B. M., Vörösmarty, C. J., Roads, J. O. & Willmott, C. J. 2004 Uncertainties in precipitation and their impacts on runoff estimates. *Journal of Climate* **17** (2), 294–304.

Fernandez, W., Vogel, R. & Sankarasubramanian, A. 2000 Regional calibration of a watershed model. *Hydrological Sciences Journal* **45** (5), 689–707.

Furlong, K. 2006 Hidden theories, troubled waters: International relations, the 'territorial trap', and the Southern African Development Community's transboundary waters. *Political Geography* **25** (4), 438–458.

Gong, L., Halldin, S. & Xu, C. Y. 2011 Global scale river routing – an efficient time delay algorithm based on HydroSHEDS high resolution hydrography. *Hydrological Processes* **25** (7), 1114–1128.

Gong, L., Widén-Nilsson, E., Halldin, S. & Xu, C. Y. 2009 Large-scale runoff routing with an aggregated network-response function. *Journal of Hydrology* **368** (1–4), 237–250.

Hagemann, S., Chen, C., Haerter, J. O., Heinke, J., Gerten, D. & Piani, C. 2011 Impact of a statistical bias correction on the

projected hydrological changes obtained from three GCMs and two hydrology models. *Journal of Hydrometeorology* **12**, 556–578.

Harris, A., Rahman, S., Hossain, F., Yarborough, L., Bagtzoglou, A. C. & Easson, G. 2007 Satellite-based flood modeling using TRMM-based rainfall products. *Sensors* **7** (12), 3416–3427.

Heyns, P. S. V. H., Patrick, M. V. & Turton, A. R. 2008 Trans boundary water resource management in southern Africa: meeting the challenge of joint planning and management in the Orange River basin. *International Journal of Water Research & Development* **24** (3), 371–383.

Huang, M., Liang, X. & Liang, Y. 2003 A transferability study of model parameters for the variable infiltration capacity land surface scheme. *Journal of Geophysical Research* **108** (8864), 1–50.

Huffman, G. J., Adler, R. F., Bolvin, D. T., Gu, G., Nelkin, E. J., Bowman, K. P., Hong, Y., Stocker, E. F. & Wolff, D. B. 2007 The TRMM multisatellite precipitation analysis: quasi-global, multi-year, combined-sensor precipitation estimates at fine scale. *Journal of Hydrometeorology* **8**, 38–55.

Huffman, G. J., Adler, R. F., Morrissey, M., Bolvin, D. T., Curtis, S., Joyce, R., cGavock, B. & Susskind, J. 2001 Global Precipitation at one-degree daily resolution from multi-satellite observations. *Journal of Hydrometeorology* **2**, 36–50.

Hughes, D. A. 2011 Regionalization of models for operational purposes in developing countries: an introduction. *Hydrology Research* **42** (5), 331–337.

Hundecha, Y. & Bárdossy, A. 2004 Modeling of the effect of land use changes on the runoff generation of a river basin through parameter regionalization of a watershed model. *Journal of Hydrology* **292** (1–4), 281–295.

Islam, M. S., Oki, T., Kanae, S., Hanasaki, N., Agata, Y. & Yoshimura, K. 2007 A grid-based assessment of global water scarcity including virtual water trading. *Water Resources Management* **21** (1), 19–33.

Jin, X., Xu, C.-Y., Zhang, Q. & Chen, Y. D. 2009 Regionalization study of a conceptual hydrological model in Dongjiang Basin, south China. *Quaternary International* **208** (1–2), 129–137.

Jung, G., Wagner, S. & Kunstmann, H. 2012 Joint climate–hydrology modeling: an impact study for the data-sparse environment of the Volta Basin in West Africa. *Hydrology Research* **43** (1–2), 231–248.

Kandji, S. T., Verchot, L. & Mackensen, J. 2006 Climate change climate and variability in southern Africa: Impacts and adaptation in the agricultural sector. World Agroforestry Centre (ICRAF) and United Nations Environment Programme (UNEP). http://agriskmanagementforum.org/doc/climate-change-climate-and-variability-southern-africa-impacts-and-adaptation-agricultural-secto.

Kendall, M. G. 1975 *Rank Correlation Methods*. Griffin, London, UK.

Kokkonen, T. S., Jakeman, A. J., Young, P. C. & Koivusalo, H. J. 2003 Predicting daily flows in ungauged catchments: model regionalization from catchment descriptors at the Coweeta Hydrologic Laboratory, North Carolina. *Hydrological Processes* **17** (11), 2219–2238.

Kumar, V. & Jain, S. K. 2011 Trends in rainfall amount and number of rainy days in river basins of India (1951–2004). *Hydrology Research* **42** (4), 290–306.

Lamb, R. & Beven, K. 1997 Using interactive recession curve analysis to specify a general catchment storage model. *Hydrology and Earth System Sciences* **1** (1), 101–113.

Layberry, R., Kniveton, D. R., Todd, M. D., Kidd, C. & Bellerby, B. J. 2006 Daily precipitation over southern Africa: a new resource for climate studies. *Journal of Hydrometeorology* **7** (1), 149–159.

Lehner, B., Döll, P., Alcamo, J., Henrichs, T. & Kaspar, F. 2006 Estimating the impact of global change on flood and drought risks in Europe: a continental, integrated analysis. *Climatic Change* **75** (3), 273–299.

Li, X. H., Zhang, Q. & Xu, C.-Y. 2012 Suitability of the TRMM satellite rainfalls in driving distributed hydrological model for water balance computations in Xinjiang catchment, Poyang lake basin. *Journal of Hydrology* **426**, 28–38.

Love, D., Uhlenbrook, S., Twomlow, S. & van der Zaag, P. 2010 Changing hydro climatic and discharge patterns in the northern Limpopo Basin, Zimbabwe. *Water SA* **36** (3), 335–350.

Mann, H. B. 1945 Nonparametric tests against trend. *Econometrica: Journal of the Econometric Society* **13** (3), 245–259.

McKay, M. D., Beckman, R. J. & Conover, W. 1979 A comparison of three methods for selecting values of input variables in the analysis of output from a computer code. *Technometrics* **21** (2), 239–245.

Milzow, C., Krogh, P. E. & Bauer-Gottwein, P. 2011 Combining satellite radar altimetry, SAR surface soil moisture and GRACE total storage changes for hydrological model calibration in a large poorly gauged catchment. *Hydrology and Earth Systems Science* **15**, 1729–1743.

Mitchell, T. D. & Jones, P. D. 2005 An improved method of constructing a database of monthly climate observations and associated high-resolution grids. *International Journal of Climatology* **25** (6), 693–712.

Montanari, A. & Toth, E. 2007 Calibration of hydrological models in the spectral domain: an opportunity for scarcely gauged basins. *Water Resources Research* **43** (5), W05434.

Nash, J. E. & Sutcliffe, J. V. 1970 River flow forecasting through conceptual models – Part 1 – A discussion of principles. *Journal of Hydrology* **10** (3), 282–290.

Ngongondo, C., Xu, C.-Y., Gottschalk, L. & Alemaw, B. 2011 Evaluation of spatial and temporal characteristics of rainfall In Malawi: a case of data scarce region. *Theoretical & Applied Climatology* 106, 79–93.

Nijssen, B., O'Donnell, G. M., Hamlet, A. F. & Lettenmaier, D. P. 2001 Hydrologic sensitivity of global rivers to climate change. *Climatic Change* **50** (1), 143–175.

Oki, T., Nishimura, T. & Dirmeyer, P. 1999 Assessment of annual runoff from land surface models using Total Runoff

Integrating Pathways (TRIP). *Journal of the Meteorological Society of Japan* **77**, 235–255.

Parajka, J., Merz, R. & Blöschl, G. 2005 A comparison of regionalisation methods for catchment model parameters. *Hydrology and Earth System Sciences* **9** (1–2), 157–171.

Piani, C., Haerter, J. & Coppola, E. 2010 Statistical bias correction for daily precipitation in regional climate models over Europe. *Theoretical and Applied Climatology* **99** (1), 187–192.

Refsgaard, J. C., van der Sluijs, J. P., Højberg, A. L. & Vanrolleghem, P. A. 2007 Uncertainty in the environmental modelling process – a framework and guidance. *Environmental Modelling and Software* **22** (11), 1543–1556.

Samaniego, L., Kumar, R. & Jackisch, C. 2011 Predictions in a data-sparse region using a regionalized grid-based hydrologic model driven by remotely sensed data. *Hydrology Research* **42** (5), 338–355.

Seibert, J. 1999 Regionalisation of parameters for a conceptual rainfall-runoff model. *Agricultural and Forest Meteorology* **98** (1), 279–293.

Shen, Y., Xiong, A., Wang, Y. & Xie, P. 2010 Performance of high-resolution satellite precipitation products over China. *Journal of Geophysical Research* **115** (D2), D02114.

Sivapalan, M., Takeuchi, K., Franks, S., Gupta, V., Karambiri, H., Lakshmi, V., Liang, X., McDonnell, J., Mendiondo, E. & O'Connell, P. 2003 IAHS Decade on Predictions in Ungauged Basins (PUB) 2003–2012: shaping an exciting future for the hydrological sciences. *Hydrological Sciences Journal* **48** (6), 857–880.

Su, F., Hong, Y. & Lettenmaier, D. P. 2008 Evaluation of TRMM multisatellite precipitation analysis (TMPA) and its utility in hydrologic prediction in the La Plata Basin. *Journal of Hydrometeorology* **9**, 622–640.

Tian, Y., Peters-Lidard, C. D., Choudhury, B. J. & Garcia, M. 2007 Multitemporal analysis of TRMM-based satellite precipitation products for land data assimilation applications. *Journal of Hydrometeorology* **8** (6), 1165–1183.

Tobin, K. J. & Bennett, M. E. 2010 Adjusting satellite precipitation data to facilitate hydrologic modeling. *Journal of Hydrometeorology* **11** (4), 966–978.

Todini, E. 2011 History and perspectives of hydrological catchment modelling. *Hydrology Research* **42** (2–3), 73–85.

Turton, A. R., Meissner, R., Mampane, P. M. & Seremo, O. 2004 A hydropolitical history of South Africa's international river basins. African Water Issues Research Unit (AWIRU) report to the Water Research Commission (WRC) report no. 1220/1/04.

Unganai, L. & Kogan, F. N. 1998 Drought monitoring and corn yield estimation in southern Africa from AVHRR data. *Remote Sensing of Environment* **63**, 219–232.

Uppala, S. M., Kållberg, P. W., Simmons, A. J., Andrae, U., Da Costa Bechtold, V., Fiorino, M., Gibson, J. K., Haseler, J., Hernandez, A., Kelly, G. A., Li, X., Onogi, K., Saarinen, S., Sokka, N., Allan, R. P., Andersson, E., Arpe, K., Balmaseda, M. A., Beljaars, A. C. M., Van De Berg, L., Bidlot, J., Bormann, N., Caires, S., Chevallier, F., Dethof, A., Dragosavac, M., Fisher, M., Fuentes, M., Hagemann, S., Hólm, E., Hoskins, B. J., Isaksen, L., Janssen, P. A. E. M., Jenne, R., Mcnally, A. P., Mahfouf, J.-F., Morcrette, J.-J., Rayner, N. A., Saunders, R. W., Simon, P., Sterl, A., Trenberth, K. A., Untch, A., Vasiljevic, D., Viterbo, P. & Woollen, J. 2005 The ERA-40 re-analysis. *Quarterly Journal of the Royal Meteorological Society* **131** (612), 2961–3012.

USGS (US Geological Survey) 1996a HYDRO 1K Elevation Derivative Database. Earth Resources Observation and Science (EROS) Data Center (EDC), Sioux Falls, South Dakota, USA. http://eros.usgs.gov/#/Find_Data/Products_and_Data_Available/gtopo30/hydro.

USGS (US Geological Survey) 1996b GTOPO30 (Global 30 Arc-Second Elevation Data Set). Earth Resources observation and Science (EROS) Data Center (EDC), Sioux Falls, South Dakota, USA. http://eros.usgs.gov/#/Find_Data/Products_and_Data_Available/gtopo30.

Vörösmarty, C. & Moore, B. 1991 Modeling basin-scale hydrology in support of physical climate and global biogeochemical Studies: an example using the Zambezi River. *Surveys in Geophysics* **12**, 271–311.

Vörösmarty, C. J., Green, P., Salisbury, J. & Lammers, R. B. 2000 Global water resources: vulnerability from climate change and population growth. *Science* **289** (5477), 284.

Weedon, G. P., Gomes, S., Viterbo, P., Österle, H., Adam, J. C., Bellouin, N., Boucher, O. & Best, M. 2010 The WATCH forcing data 1958–2001: a meteorological forcing dataset for land surface-and hydrological- Rep., WATCH Tech. Rep. 22, pp. 41. Available from: http://www.eu-watch.org/publications/technical-reports (accessed September 2012).

Weedon, G. P., Gomes, S., Viterbo, P., Shuttleworth, W., Blyth, E., Österle, H., Adam, J., Bellouin, N., Boucher, O. & Best, M. 2011 Creation of the WATCH Forcing Data and its use to assess global and regional reference crop evaporation over land during the twentieth century. *Journal of Hydrometeorology* **12** (5), 823–848.

Westerberg, I., Guerrero, J., Younger, P., Beven, K., Seibert, J., Halldin, S., Freer, J. & Xu, C.-Y. 2011 Calibration of hydrological models using flow-duration curves. *Hydrology and Earth System Sciences* **15**, 2205–2227.

Widen-Nilsson, E., Gong, L., Halldin, S. & Xu, C.-Y. 2009 Model performance and parameter behavior for varying time aggregations and evaluation criteria in the WASMOD-M global water balance model. *Water Resources Research* **45** (5), W05418.

Winsemius, H., Schaefli, B., Montanari, A. & Savenije, H. 2009 On the calibration of hydrological models in ungauged basins: a framework for integrating hard and soft hydrological information. *Water Resources Research* **45** (W12422), W12422.

Xu, C.-Y. 1999a Estimation of parameters of a conceptual water balance model for ungauged catchments. *Water Resources Management* **13** (5), 353–368.

Xu, C.-Y. 1999b Operational testing of a water balance model for predicting climate change impacts. *Agricultural and Forest Meteorology* **98–99**, 295–304.

Xu, C.-Y. 2001 Statistical analysis of parameters and residuals of a conceptual water balance model – methodology and case study. *Water Resources Management* **15** (2), 75–92.

Xu, C.-Y. 2002 WASMOD-The Water and Snow balance MODelling system. In: *Mathematical Models of Small Watershed Hydrology and Applications* (V. P. Singh & D. K. Frevert, eds). Water Resources Publications, Chelsea, Michigan, USA, pp. 555–590.

Xu, C.-Y. 2003 Testing the transferability of regression equations derived from small sub-catchments to large area in central Sweden. *Hydrology and Earth System Sciences* **7** (3), 317–324.

Xu, C.-Y., Seibert, J. & Halldin, S. 1996 Regional water balance modelling in the NOPEX area: development and application of monthly water balance models. *Journal of Hydrology* **180**, 211–236.

Yadav, M., Wagener, T. & Gupta, H. 2007 Regionalization of constraints on expected watershed response behavior for improved predictions in ungauged basins. *Advances in Water Resources* **30** (8), 1756–1774.

Yang, C., Yu, Z., Hao, Z., Zhang, J. & Zhu, J. 2012 Impact of climate change on flood and drought events in Huaihe River Basin, China. *Hydrology Research* **43** (1–2), 14–22.

Yilmaz, K. K., Gupta, H. V. & Wagener, T. 2008 A process-based diagnostic approach to model evaluation: application to the NWS distributed hydrologic model. *Water Resources Research* **44** (9), W09417.

Yu, P. S. & Yang, T. C. 2000 Using synthetic flow duration curves for rainfall–runoff model calibration at ungauged sites. *Hydrological Processes* **14** (1), 117–133.

Zhang, Q., Xu, C.-Y., Zhang, Z., Chen, Y., Liu, C. & Lin, H. 2008 Spatial and temporal variability of precipitation maxima during 1960–2005 in the Yangtze River basin and possible association with large-scale circulation. *Journal of Hydrology* **353** (3–4), 215–227.

Zhang, Q., Xu, C.-Y., Zhang, Z., Chen, Y. & Liu, C. L. 2009 Spatial and temporal variability of precipitation over China 1951–2005. *Theoretical and Applied Climatology* **95** (1), 53–68.

Zhu, T. & Ringler, C. 2010 Climate change implications for water resources in the Limpopo River Basin. International Food Policy Research Unit, Discussion Paper 00961.

First received 15 November 2011; accepted in revised form 1 March 2012. Available online 13 October 2012